environmental sciences proceedings

MDPI

Proceeding Paper

Automated Application for Visualizing Rainfall and Hail Estimations Derived from an Algorithm Based on Meteosat Multispectral Image Data †

Niki Papavasileiou and Stavros Kolios *

Department of Aerospace Science and Technology, Faculty of Sciences, National Kapodistrian University of Athens, 34400 Psachna, Greece; nickypap01@gmail.com

* Correspondence: skolios@aerospace.uoa.gr

† Presented at the 6th International Electronic Conference on Atmospheric Sciences, 15–30 October 2023; Available online: https://ecas2023.sciforum.net/.

Abstract: The scope of this study is an attempt to develop an automated visualization module to monitor rainfall and hail estimations in real-time, highlighting areas with potential risk from extreme weather phenomena. The rainfall/hail products are provided by a known satellite-based algorithm that uses exclusively Meteosat multispectral images. The application is fully automated, written in the Python programming environment using open-source libraries, and provides colored graphs about the spatial variation of the examined parameters with the same temporal resolution as the Meteosat imagery. Additional functions of this application include warnings for extreme situations each time predefined threshold values are exceeded, as well as geographical areas that are vulnerable to heavy rainfall and/or hail occurrences. This application is a pilot operating over the Greek periphery. Also, there is a capability to create small video animations for the spatiotemporal evolution of the rainfall and hail estimations up to 6 h before the latest available satellite images.

Keywords: visualization; meteosat; rainfall estimations; automated application; real-time monitoring

Citation: Papavasileiou, N.; Kolios, S. Automated Application for Visualizing Rainfall and Hail Estimations Derived from an Algorithm Based on Meteosat Multispectral Image Data. *Environ. Sci. Proc.* **2023**, *27*, 8. https://doi.org/10.3390/ecas2023-15383

Academic Editor: Teodoro Georgiadis

Published: 26 October 2023

1. Introduction

Extreme weather events are dangerous to lives, properties, and infrastructures. Their accurate monitoring needs innovative approaches and still remains a challenging research issue. By harnessing the capabilities of meteorological satellites, specifically Meteosat, it is capable of the development of precise algorithms for estimating meteorological parameters and their subsequent visualization [1–3]. Such monitoring capabilities not only offer timely insights but also present the potential to mitigate damage to infrastructure and private properties caused by extreme weather [4,5].

This study primarily focuses on two meteorological phenomena: rainfall and hail. Rainfall is the process by which water droplets precipitate from atmospheric clouds, whereas hail involves the formation of solid ice within storm systems. Both these meteorological events can have profound impacts. Accurate estimations and forecasts of rainfall and hail serve as crucial tools in disaster preparedness and response. While rainfall can lead to flooding, landslides, and disruptions in urban areas, hail can inflict significant damage to crops, vehicles, and structures [5–11]. The precise and real-time monitoring of these parameters can aid in issuing early warnings, allowing for preemptive measures, and thereby reducing potential harm.

2. Data and Methods

For the scope of this study, data from a satellite-based rain estimation algorithm have been used. The algorithm of Kolios, 2023, first distinguishes rain/non-rain pixels based on a thresholding method. Then, it uses the Brightness Temperature from Meteosat-11

in five spectral bands from 6.0 to 12.0 m (channels 5–7, 9 and 10) to calculate pixel-wise rain intensity [12,13]. Moreover, the algorithm automatically provides data every 15 min, contingent on its availability from the satellite.

The datasets encompass a range of vital information, including latitude (LAT), longitude (LON), precipitation (Prec), and hail (Hail) data. Prior to analysis, a comprehensive data cleaning process is undertaken using the Pandas library—a powerful tool in data manipulation and analysis—to ensure reliability and precision [14]. This involves the removal of invalid or unhelpful entries, such as negative estimation values and any missing or null values.

Following this preprocessing, the next step involves the visualization of the data. Leveraging libraries Matplotlib—a plotting library and Cartopy—a library designed for geospatial data visualization [15,16], the data are transformed into contour maps, offering an optimal representation of the phenomena. These maps are enhanced with a color-bar, further clarifying the visualized data for improved comprehension. It is imperative to note that the visualization is capable of real-time updates. Whenever new data becomes available, an automated process routinely checks and processes these data using the previously described methods.

Upon successful visualization of the data, it is crucial to detect hazardous phenomena. This identification is achieved using the DBSCAN clustering algorithm [17], which is employed after discerning 'danger points' through a thresholding technique. This specific algorithm detects clusters of high-risk points by analyzing their spatial density. After the clustering, the Principal Component Analysis (PCA) is employed to extract key characteristics of each cluster, such as its center, minor axis, and major axis. Utilizing Equation (1):

$$\frac{x^2}{a^2} + \frac{y^2}{b^2} \leq 1 \quad (1)$$

where,

x, y are the transformed coordinates;

a is the semi-major axis;

b is the semi-minor axis.

The points within each cluster are then generated. Subsequently, these points are matched with city coordinates from corresponding datasets, updating the information and alerts about cities impacted by the weather phenomena.

For a more in-depth understanding, the final feature offers short video animations depicting the spatiotemporal evolution of rainfall and hail estimates up to 6 h before the last available satellite images. Contour maps are produced for each time point, and with the aid of Library Pillow [18], these are seamlessly integrated into a dynamic animation.

3. Results and Discussion

As shown in Figure 1, using a varied palette, the color bar accurately maps rainfall intensities ranging from 0 to 29 mm/hr. The contour maps, through their distinct color variations, clarify these intensities, providing viewers with a clear sense of the meteorological conditions. The data from which this illustration is derived is for the timestamp 03/06/2023 at 15:15. Such visual tools, because of their clarity, are catalytic for understanding specific atmospheric phenomena.

The results of the visualization and detection of heavy rainfall, derived from the MWAVE (METEOSAT Weather Alert and Visualization Environment) application, can be seen in Figure 2. The Figure depicts detected intense localized precipitation on 03/06/2023 at 13:30, impacting several regions within Greece and adjacent countries. Following successful detection, the local phenomena are effectively delineated and represented within ellipses. Pertinent information and updates regarding the affected cities are presented on the left side of the graphical interface. The results indicate cities situated in regions such as Western Macedonia, Peloponnese, and Central Greece.

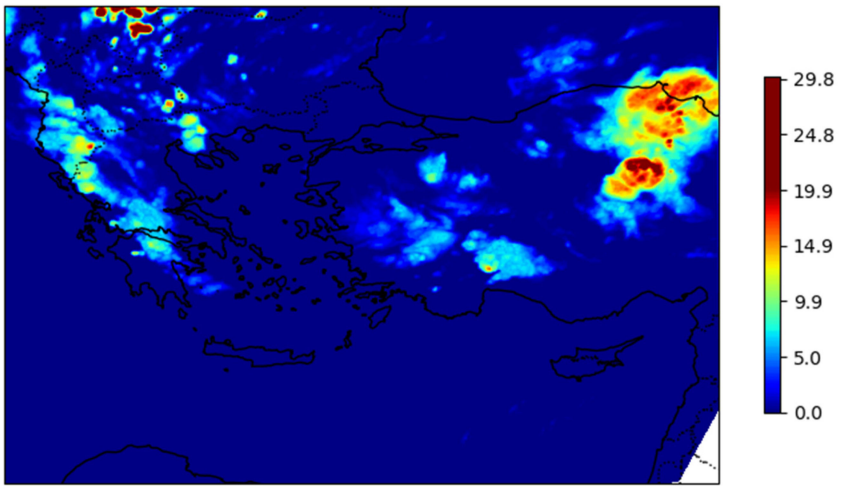

Figure 1. Visualization of rainfall data on a contour map for the date 03/06/2023 15:15.

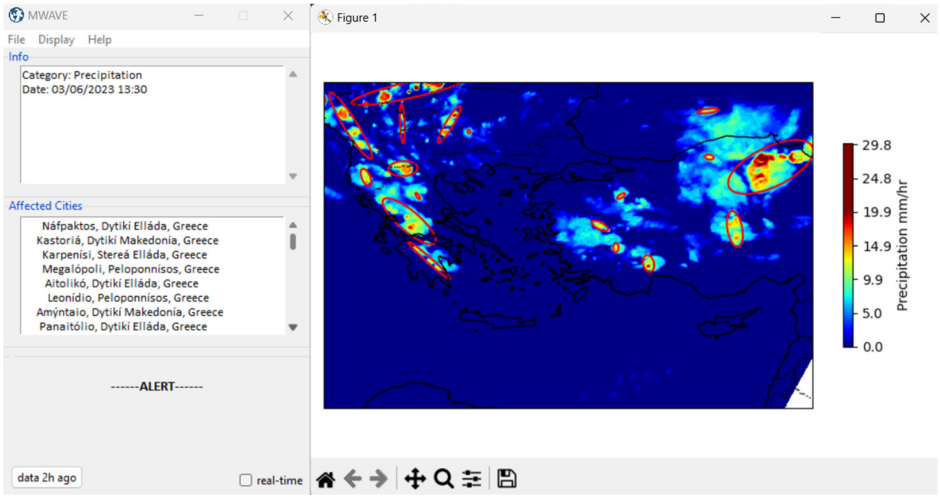

Figure 2. Screenshot of the graphical environment of the application to detect heavy rainfall for the date 03/06/2023 13:30.

In a further exploration of the data, Figure 3 delves into the detection of hail phenomena for the timestamp of 03/06/2023 at 15:15. Notably, no dangerous hail phenomena are identified during this interval. This absence of high-risk hail activity is clearly reflected in the information section of the graphical interface. If there had been any significant hail occurrences, they would have been highlighted within ellipses, and pertinent details and alerts regarding affected regions would be displayed on the left side of the interface. For the given timestamp, the depicted regions exhibit no discernible hail threats of significance. At this point, it noted that the absence of hail risk is referred only in the randomly selected time/day interval. The general accuracy of the product on hail, precipitation, and AOD detection is presented in the study [12,13,19], respectively.

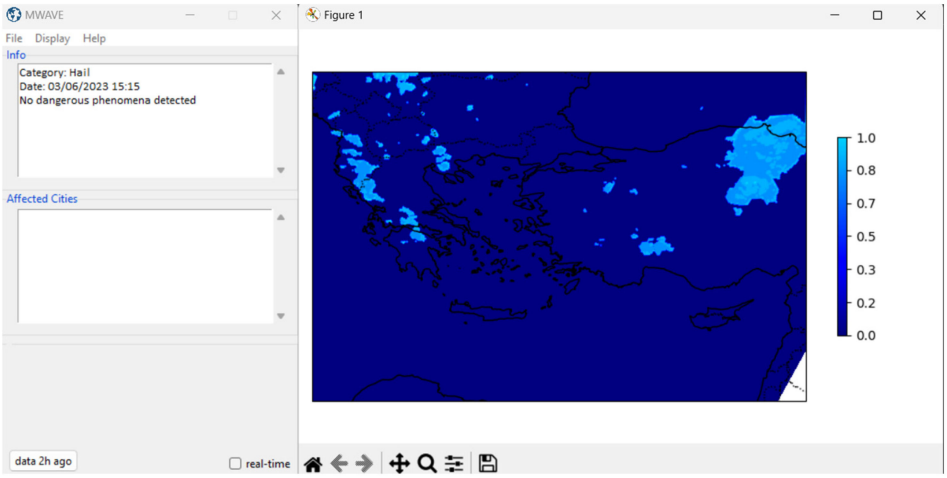

Figure 3. Screenshot of the graphical environment of the application to detect hail for the date 03/06/2023 15:15.

4. Conclusions

This study showcases the employment of Meteosat multispectral imagery for the real-time visualization of rainfall and hail estimations over Greece. Through an automated Python-based application, the detection feature highlights the system's capabilities to detect threats and issue real-time alerts. The results demonstrated the ability of the system to describe rainfall intensities with high accuracy, as shown in Figures 1 and 2, providing information on regional impacts across Greece and neighboring countries. In particular, Figure 3 revealed the absence of significant hail threats during the period analyzed, highlighting the value of the tool for both detecting threats and confirming favorable conditions. Overall, the visual representations, enhanced by a color palette, provide an intuitive understanding of meteorological conditions, demonstrating that they contribute to timely and informed decision-making.

Subsequent versions of the application are projected to incorporate additional features, notably nowcasting capabilities. Such enhancements are expected to provide even more immediate and precise meteorological insights. The integration of these advancements aims to further refine the tool's accuracy and bolster its utility in real-time weather monitoring and informed decision-making.

Author Contributions: Conceptualization, S.K.; methodology, S.K.; software, S.K. and N.P.; validation, S.K. and N.P.; formal analysis, S.K. and N.P.; investigation, S.K.; resources, N.P.; data curation, S.K. and N.P.; writing—original draft preparation, S.K.; writing—review and editing, S.K. and N.P.; visualization, N.P.; supervision, S.K.; project administration, S.K. All authors have read and agreed to the published version of the manuscript.

Funding: This research received no external funding.

Institutional Review Board Statement: Not applicable.

Informed Consent Statement: Not applicable.

Data Availability Statement: The data presented in this study are available on request from the corresponding author. The data are not publicly available due to research restrictions and relative terms and conditions.

Acknowledgments: The authors acknowledge the providers of all the different datasets used in this study: EUMETSAT (European Organization for the Exploitation of Meteorological Satellites) for the free provision of the Meteosat multispectral satellite images (raw datasets) and SimpleMaps for providing dataset information on cities.

Conflicts of Interest: The authors declare no conflicts of interest.

References

1. Scarino, B.; Itterly, K.; Bedka, K.; Homeyer, C.R.; Allen, J.; Bang, S.; Cecil, D. Deriving Severe Hail Likelihood from Satellite Observations and Model Reanalysis Parameters Using a Deep Neural Network. *Artif. Intell. Earth Syst.* **2023**, *2*, 220042. [CrossRef]
2. Batbold, C.; Yumimoto, K.; Chonokhuu, S.; Byambaa, B.; Avirmed, B.; Ganbat, S.; Kaneyasu, N.; Matsumi, Y.; Yasunari, T.J.; Taniguchi, K.; et al. Spatiotemporal Dispersion of Local-Scale Dust from the Erdenet Mine in Mongolia Detected by Himawari-8 Geostationary Satellite. *SOLA* **2022**, *18*, 225–230. [CrossRef]
3. Xu, G.; Zhong, X. Real-Time Wildfire Detection and Tracking in Australia Using Geostationary Satellite: Himawari-8. *Remote Sens. Lett.* **2017**, *8*, 1052–1061. [CrossRef]
4. Gosset, M.; Dibi-Anoh, P.A.; Schumann, G.; Hostache, R.; Paris, A.; Zahiri, E.-P.; Kacou, M.; Gal, L. Hydrometeorological Extreme Events in Africa: The Role of Satellite Observations for Monitoring Pluvial and Fluvial Flood Risk. *Surv. Geophys.* **2023**, *44*, 197–223. [CrossRef]
5. Jeyaseelan, A. Droughts and Floods Assessment and Monitoring using Remote Sensing and GIS. In Proceedings of Satellite Remote Sensing and GIS Applications in Agricultural Meteorology, Dehra Dun, India, 7–11 July 2003; pp. 291–313.
6. Marengo, J.A.; Alves, L.M.; Ambrizzi, T.; Young, A.; Barreto, N.J.C.; Ramos, A.M. Trends in Extreme Rainfall and Hydrogeometeorological Disasters in the Metropolitan Area of São Paulo: A Review. *Ann. N. Y. Acad. Sci.* **2020**, *1472*, 5–20. [CrossRef] [PubMed]
7. Martha, T.; Roy, P.; Khanna, K.; Kotteeswaran, M.; vinod Kumar, K. Landslides Mapped from Satellite Data in the Western Ghats of Indian Peninsula after the August 2018 Excess Rainfall. *Curr. Sci.* **2019**, *117*, 804–812. [CrossRef]
8. Zhou, J.; Bgood, J.; Shelton, S.; Holden, Z.; Sankaran, S. Aerial Multispectral Imaging for Crop Hail Damage Assessment in Potato. *Comput. Electron. Agric.* **2016**, *127*, 406–412. [CrossRef]
9. Peters, A.J.; Griffin, S.C.; Viña, A.; Ji, L. Use of Remotely Sensed Data for Assessing Crop Hail Damage. *Photogramm. Eng. Remote Sens.* **2000**, *66*, 1349–1355.
10. Hohl, R.; Schiesser, H.-H.; Knepper, I. The Use of Weather Radars to Estimate Hail Damage to Automobiles: An Exploratory Study in Switzerland. *Atmos. Res.* **2002**, *61*, 215–238. [CrossRef]
11. Hohl, R.; Schiesser, H.-H.; Aller, D. Hailfall: The Relationship between Radar-Derived Hail Kinetic Energy and Hail Damage to Buildings. *Atmos. Res.* **2002**, *63*, 177–207. [CrossRef]
12. Kolios, S. Hail Detection from Meteosat Satellite Imagery Using a Deep Learning Neural Network and a New Remote Sensing Index. *Adv. Space Res.* **2023**, *72*, 3009–3021. [CrossRef]
13. Kolios, S.; Hatzianastassiou, N.; Lolis, C.J.; Bartzokas, A. Accuracy Assessment of a Satellite-Based Rain Estimation Algorithm Using a Network of Meteorological Stations over Epirus Region, Greece. *Atmosphere* **2022**, *13*, 1286. [CrossRef]
14. The Pandas Development Team. Pandas-Dev/Pandas: Pandas. 2020. Available online: https://zenodo.org/records/10426137 (accessed on 27 September 2023).
15. Hunter, J. Matplotlib: A 2D Graphics Environment. *Comput. Sci. Eng.* **2007**, *9*, 90–95. [CrossRef]
16. Office, M. Cartopy: A cartographic python library with a Matplotlib interface. Exeter, Devon, v0.16 edition 2010–2017. Available online: http://scitools.org.uk/cartopy (accessed on 27 September 2023).
17. Pedregosa, F.; Varoquaux, G.; Gramfort, A.; Michel, V.; Thirion, B.; Grisel, O.; Blondel, M.; Prettenhofer, P.; Weiss, R.; Dubourg, V.; et al. Scikit-Learn: Machine Learning in Python. Machine Learning in Python. *J. Mach. Learn. Res.* **2011**, *12*, 2825–2830.
18. Clark, A. Pillow (PIL Fork) Documentation. Available online: https://buildmedia.readthedocs.org/media/pdf/pillow/latest/pillow.pdf (accessed on 27 September 2023).
19. Kolios, S.; Hatzianastassiou, N. Quantitative Aerosol Optical Depth detection during dust outbreaks from Meteosat imagery using an Artificial Neural Network model. *Remote Sens.* **2019**, *11*, 1022. [CrossRef]